P2.31

CALIBRATION OF GOES WATER VAPOR SPATIAL GRADIENTS WITH TROPOPAUSE FOLDING EVENTS

Anthony J. Wimmers* and Jennie L. Moody
University of Virginia, Charlottesville, Virginia

1. INTRODUCTION

The mixing of stratospheric air into the troposphere, or stratosphere-troposphere exchange (STE), is an important behavior of the atmosphere because of its dynamic and as well as chemical effects. STE delivers stratospheric air with high potential vorticity (PV) into the troposphere, which can be directly responsible for subsequent cyclogenesis (Hoskins et al., 1985). The extreme dryness of stratospheric air delivered into the troposphere has obvious affects on condensation, evaporation and radiative energy balance. Furthermore, the transport of ozone-rich stratospheric air into the troposphere plays an important role in the trace gas chemistry of the troposphere, which in turn can affect climate, human health and economic development.

Tropopause folding is a major mechanism of STE in the middle and high latitudes. Although its primary features have been captured effectively by computer models of midlatitude cyclone life cycles, recent measurements from the 2000 TOPSE (Tropospheric Ozone Production about the Spring Equinox) campaign suggest that tropopause folding occurs far more often than just within the limited scope of midlatitude cyclones. During the four-month period of aircraft flights, every crossing of an upper-tropospheric air mass boundary (observed in the satellite imagery) corresponded in time to a lidar-observed cross-section of tropopause folding (Wimmers et al., 2002). The Altered Water Vapor (AWV) product was the primary form of satellite imagery used in this study, because of its ability to distinguish the differences in specific humidity between air masses in the upper troposphere. However, these observations of tropopause folding at upper-level air mass boundaries were only qualitative.

2. OBJECTIVE

The objective of this study is to describe a quantitative relationship between AWV-observed humidity gradients and lidar-observed tropopause folding. The ten cases of tropopause folding described in Wimmers et al. (2002) are revisited here as cases for examining the quantitative spatial gradients in the AWV imagery. There is a good reason to expect that AWV gradients above a "threshold" gradient magnitude will signify important upper-level air mass boundaries, and thus correspond directly to tropopause folding events. This study attempts to quantify that threshold. This is important because an empirically derived threshold gradient magnitude could be scaled up to the large temporal and spatial domain of the AWV product (equal to the domain of the GOES water vapor channel) in order to reach better conclusions about the distribution of tropopause folding across the globe.

3. AWV GRADIENTS

The AWV product is a linear modification of the GOES water vapor channel imagery that depicts variations in specific humidity. Its main benefit is the depiction of a nearly conservative tracer (water vapor) rather than a signal (brightness temperature) that varies with temperature and zenith angle as well as water vapor. The sensitivity of the AWV product is between about 200 and 450 hPa, with a peak at 300 hPa, which is beneficial for viewing moisture patterns around the height of the tropopause (Wimmers and Moody, 2001).

The method for determining the proper spatial gradients in AWV imagery is summarized as follows. First, the AWV imagery was remapped to an equirectangular grid because of its straightforward aspect ratio between the latitudinal and longitudinal directions. Second, a gaussian filter was applied to the image. This is akin to "blurring" or "smoothing" the image in order to emphasize the larger-scale gradients and de-emphasize the effects of features such as thin cirrus clouds along air mass boundaries. The size of the gaussian filter is a parameter to be tested in the study. Third, an empirically determined cloud mask is applied to the imagery by truncating the humidity derived by the AWV product at a specified upper limit. Fourth, a discrete spatial gradient operator is applied to the image, with consideration for the difference in distances between the latitudinal and longitudinal directions on the map. Finally, the gradient magnitude is determined as a square root of the sum of the squares of the longitudinal and latitudinal gradient vector elements.

4. DETERMINING A THRESHOLD FROM TRANSECT DATA

AWV gradient magnitude images (Plate 1) were matched with the ten TOPSE flight transects under investigation (Plate 2). These images were then sampled along the path of the flight track, creating a transect of AWV gradient magnitude ("gradient transects") to be compared to its corresponding lidar cross-section (Plate 3). In the analysis of these gradient

* *Corresponding author address*: Anthony J. Wimmers, Dept. of Environmental Sciences, Clark Hall, Univ. of Virginia, Charlottesville, VA, 22903; email: wimmers@virginia.edu

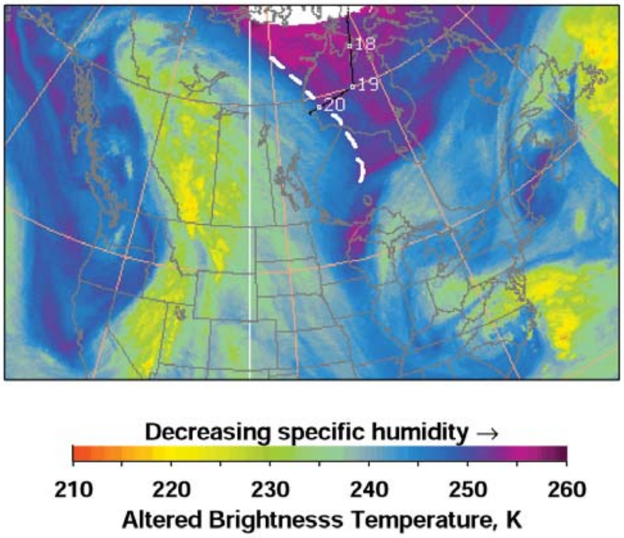

Plate 1. Altered Water Vapor image from 1800 UTC 28 April 2000; flight track, black line; time of flight (UTC), white text; strong humidity gradient encountered by aircraft, dashed white line.

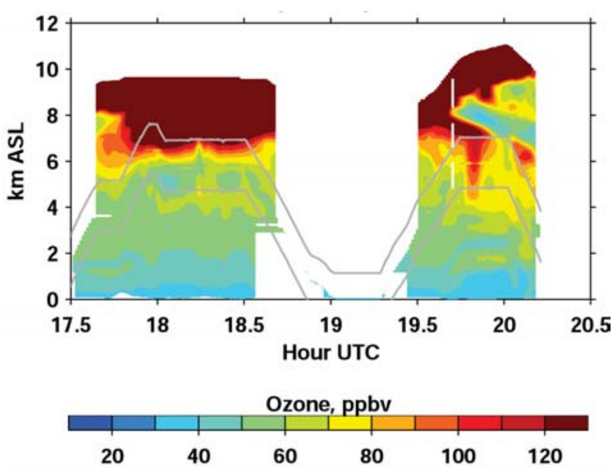

Plate 2. Differential Absorption Lidar (DIAL) ozone transect from the flight shown in Plate 1. Gray lines in DIAL plots represent the upper and lower limits of the downward and upward lidar, respectively (inside these lines, the data is interpolated). White dashed line at ~19.7 hours UTC highlights the time of the tropopause fold opening.

transects, each "significant" peak (a maximum in the gradient magnitude) was found to coincide closely in time with the opening of a tropopause fold. Stated more precisely, every peak in the gradient magnitude plots above a certain threshold value corresponded in time to a tropopause fold. The threshold that best separated the "significant" gradients from the "insignificant" gradients was 3.2 K per standard degree, where a standard degree is the distance between degrees latitude (111

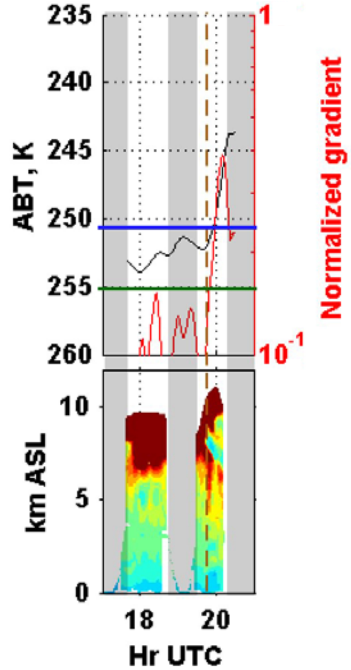

Plate 3. AWV transect from the flight depicted in Plates 1 and 2; smoothed altered brightness temperature (ABT) (y-axis scale on right), black line; ABT gradient magnitude normalized to the maximum value sampled in TOPSE (y-axis scale on left), red line; upper threshold, blue horizontal line; lower threshold, green horizontal line; DIAL transects of ozone, lower row; time periods of no DIAL data, gray bars; incident of tropopause folding, brown dashed line.

km). This threshold value is the average of the upper threshold and lower threshold shown in Plate 3. Furthermore, the gaussian filter that produced an optimal difference between significant gradients and insignificant gradients had a full width at half-maximum of about 0.60 standard degrees, or ~70 km. These two parameters (threshold gradient and smoothing filter width) can be used to optimize a statistical model that estimates the locations of tropopause folding throughout an AWV image.

5. PARAMETERIZATION OF FOLDING LENGTH

The length of the tropopause folds from the TOPSE measurements can be estimated from the lidar images after taking into account the angle at which the flight track intersected the fold. Using a subset of lidar cross-sections in which the entire fold was sampled end-to-end, the average length of the tropopause folds encountered in the TOPSE campaign was 2 standard degrees, or ~222 km. However, this result is not robust because of the limited number of samples from which it was taken. Contrary to expectations, the folding length had no relationship to the magnitude of the AWV gradient to which it corresponded, even though AWV gradient magnitude describes the "contrast" between air mass boundaries, which should bear some relationship to the mechanisms that intensify tropopause folding. We hypothesize that this lack of a relationship has two reasons: first, the folds were observed in different stages of growth and the lifetime of the fold likely affects its size as much as the causes of its growth; second, uneven chemical destruction of intruded ozone in the free troposphere may have prevented the ozone lidar measurement from capturing the full size of many of the folds.

When this AWV-based parameterization of tropopause folding is scaled up to the domain of the GOES imager, two features become immediately apparent (Plate 4). First, the signatures of tropopause folding are ubiquitous across the middle and high latitudes. Although the estimated folding length is not robust, this example confirms that the coverage of tropopause folding is much greater than what would be indicated by a reanalysis or chemical transport model. Second, the occurrence of folding is almost contiguous around the upper-tropospheric perimeter of the polar air mass, suggesting a nearly continuous transport of stratospheric air all across the polar tropopause break, at least during the February to May period of the study.

6. CONCLUSION

The spatial gradient of the AWV product, above a determined threshold, corresponds closely to upper air mass boundaries where tropopause folding and STE occurs. When scaled up to the domain of the GOES satellite imagery, the occurrence of tropopause folding indicated by AWV gradients is significantly more common than has been suggested by other methods of estimation. This result can be used to further explore the spatial and temporal patterns of tropopause folding throughout the GOES viewing domain from a unique and valuable observation-based perspective.

7. ACKNOWLEDGMENTS

Support for this work was provided by the National Science Foundation under the TOPSE project, grant OPP-9908840 and by NOAA/NESDIS (award number NA96ECO011).

8. REFERENCES

Hoskins, B.J., M.E. McIntyre, and A.W. Robertson, 1985: On the use and significance of isentropic potential vorticity maps, *Q. J. R.. Meteorol. Soc.*, **111** (470), 877-946.

Wimmers, A.J., and J.L. Moody, 2001: A fixed-layer estimation of upper tropospheric specific humidity from the GOES water vapor channel: Parameterization and validation of the altered brightness temperature product, *J. Geophys. Res.*, **106** (D15), 17115-17132.

Wimmers, A.J., J.L. Moody, E.V. Browell, J.W. Hair, W.B. Grant, C.F. Butler, M.A. Fenn, C.C. Schmidt, J. Li, and B.A. Ridley, 2002: Signatures of tropopause folding in satellite imagery, *J. Geophys. Res.*, *in press*.

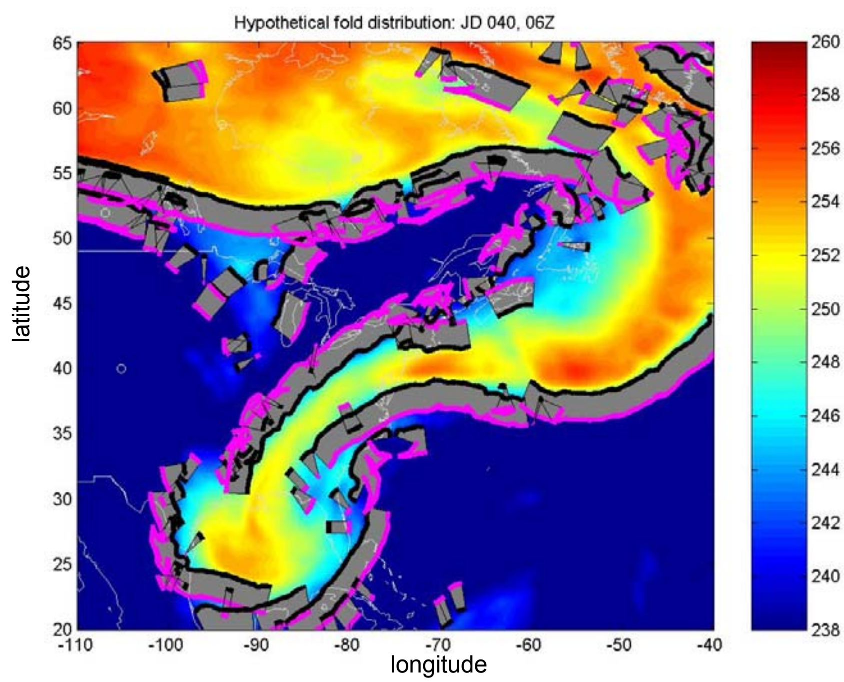

Plate 4. Hypothetical coverage of tropopause folds based on AWV imagery from 0600 UTC 6 Feb 2000. Background image is smoothed altered brightness temperature, truncated at 238 K (colorscale is in units of degrees K). "Opening" of the tropopause folds at spatial gradients exceeding the 3.2 K/degree threshold, black lines; "ending" of the tropopause folds at a distance out of 2 standard degrees (222 km), magenta lines; total fold coverage, gray area. Note there is a change in color scale from Plate 1.